AMERICAN SOCIETY FOR MICROBIOLOGY | Applied and Environmental Microbiology®

ENVIRONMENTAL MICROBIOLOGY

High-Level Abundances of *Methanobacteriales* and *Syntrophobacterales* May Help To Prevent Corrosion of Metal Sheet Piles

Michiel H. in 't Zandt,[a,b] Nardy Kip,[c,f] Jeroen Frank,[a,d] Stefan Jansen,[e] Johannes A. van Veen,[c] Mike S. M. Jetten,[a,b,d] Cornelia U. Welte[a,d]

[a]Department of Microbiology, Institute for Water and Wetland Research, Radboud University, Nijmegen, the Netherlands
[b]Netherlands Earth System Science Center, Utrecht University, Utrecht, the Netherlands
[c]Department of Microbial Ecology, Netherlands Institute of Ecology (NIOO-KNAW), Wageningen, the Netherlands
[d]Soehngen Institute of Anaerobic Microbiology, Radboud University, Nijmegen, the Netherlands
[e]Deltares, Utrecht, the Netherlands
[f]Institute of Applied Biosciences and Chemistry, HAN University of Applied Sciences, Nijmegen, the Netherlands

ABSTRACT Iron sheet piles are widely used in flood protection, dike construction, and river bank reinforcement. Their corrosion leads to gradual deterioration and often makes replacement necessary. Natural deposit layers on these sheet piles can prevent degradation and significantly increase their life span. However, little is known about the mechanisms of natural protective layer formation. Here, we studied the microbially diverse populations of corrosion-protective deposit layers on iron sheet piles at the Gouderak pumping station in Zuid-Holland, the Netherlands. Deposit layers, surrounding sediment and top sediment samples were analyzed for soil physicochemical parameters, microbially diverse populations, and metabolic potential. Methanogens appeared to be enriched 18-fold in the deposit layers. After sequencing, metagenome assembly and binning, we obtained four nearly complete draft genomes of microorganisms (*Methanobacteriales*, two *Coriobacteriales*, and *Syntrophobacterales*) that were highly enriched in the deposit layers, strongly indicating a potential role in corrosion protection. *Coriobacteriales* and *Syntrophobacterales* could be part of a microbial food web degrading organic matter to supply methanogenic substrates. Methane-producing *Methanobacteriales* could metabolize iron, which may initially lead to mild corrosion but potentially stimulates the formation of a carbonate-rich protective deposit layer in the long term. In addition, *Methanobacteriales* and *Coriobacteriales* have the potential to interact with metal surfaces via direct interspecies or extracellular electron transfer. In conclusion, our study provides valuable insights into microbial populations involved in iron corrosion protection and potentially enables the development of novel strategies for *in situ* screening of iron sheet piles in order to reduce risks and develop more sustainable replacement practices.

IMPORTANCE Iron sheet piles are widely used to reinforce dikes and river banks. Damage due to iron corrosion poses a significant safety risk and has significant economic impact. Different groups of microorganisms are known to either stimulate or inhibit the corrosion process. Recently, natural corrosion-protective deposit layers were found on sheet piles. Analyses of the microbial composition indicated a potential role for methane-producing archaea. However, the full metabolic potential of the microbial communities within these protective layers has not been determined. The significance of this work lies in the reconstruction of the microbial food web of natural corrosion-protective layers isolated from noncorroding metal sheet piles. With this work, we provide insights into the microbiological mechanisms that potentially

Citation in 't Zandt MH, Kip N, Frank J, Jansen S, van Veen JA, Jetten MSM, Welte CU. 2019. High-level abundances of *Methanobacteriales* and *Syntrophobacterales* may help to prevent corrosion of metal sheet piles. Appl Environ Microbiol 85:e01369-19. https://doi.org/10.1128/AEM.01369-19.

Editor Shuang-Jiang Liu, Chinese Academy of Sciences

Address correspondence to Cornelia U. Welte, c.welte@science.ru.nl.

Received 18 June 2019
Accepted 11 August 2019
Accepted manuscript posted online 16 August 2019
Published 1 October 2019

promote corrosion protection in freshwater ecosystems. Our findings could support the development of screening protocols to assess the integrity of iron sheet piles to decide whether replacement is required.

KEYWORDS corrosion protection, iron sheet piles, methanogens, organic compound degradation

Metal constructions are widely used in waterways, such as wharf structures, pile foundations, and metal sheet piles. Their corrosion poses significant safety risks and has significant economic impact, with total costs estimated at 2.2 trillion dollars per year globally (1). Microbially influenced corrosion contributes to at least 10 to 20% of total corrosion damage, which emphasizes the relevance of this process (2, 3). Microorganisms influence metal corrosion both under oxic and anoxic conditions by changing the chemical environment through metabolic processes and biofilm formation on metal surfaces (1, 4). Under oxic conditions, both abiotic and microbial processes lead to the formation of hematite (Fe_2O_3) and ferric hydroxide [$Fe(OH)_3$] and active acidification of the environment, which increases corrosion rates (5). Under anoxic conditions the iron corrosion is largely influenced by microbial activity (6). In marine environments, sulfate-reducing bacteria induce iron corrosion under electroconductive conditions, which is a major issue in pipeline steel (6, 7). In anoxic freshwater environments, sulfate reducing *Desulfovibrio* species can cause corrosion of metal surfaces when sulfate is abundant (12.5 to 35.2 mM), as shown under laboratory conditions (8–10). Under low-sulfate conditions, as for most freshwater ecosystems, iron oxidation mainly proceeds via the formation of ferrous hydroxide [$Fe(OH)_2$] that is transformed into magnetite (Fe_3O_4) with the formation of H_2 as main electron sink (11).

In addition to their role in corrosion, microorganisms have also been found to potentially be involved in corrosion protection through the development of corrosion-protective layers (CPLs). A Dutch study indicated that such natural CPLs were associated with corrosion inhibition in organic-rich freshwater environments in five freshwater field sites (12). CPLs are formed by multispecies biofilms which likely exert several protective mechanisms, including the removal of corrosive substances, e.g., the removal of oxygen through aerobic respiration (13); growth inhibition of corrosion causing microbes, e.g., through antimicrobial production by noncorrosive microorganisms (14); and the formation of a corrosion protective layer, e.g., through overproduction of extracellular polymeric substances and mineral precipitation (12, 15). Natural CPLs are therefore a mixture of mineral and biological matrices and are a promising sustainable alternative to current more harsh corrosion inhibition methods. The layer stability is, however, highly pH dependent, and the pH in turn is dependent on microbial processes. The hydrogen (H_2) produced through corrosion can be an energy source for many microorganisms, including hydrogenotrophic methanogenic archaea that convert this substrate to methane (CH_4), a potent greenhouse gas (16). However, the composition of microbial communities within natural CPLs is largely unknown. Associating chemical processes with microbial communities is essential in determining the formation and dynamics of corrosion-protective layers.

We studied 4-m-deep iron sheet piles at a pumping station in Gouderak, Zuid-Holland, the Netherlands. The Gouderak pump station was constructed in 1866 and pushes excess water out of the Stolwijksche Boezem into the river Hollandse IJssel. The iron sheet piles protect the dikes and banks from erosion. The average life span of these sheet piles ranges between 50 and 100 years. Their replacement is both a risky and expensive endeavor. At Gouderak, sheet piles were replaced preemptively 50 years after installment. Previous studies of iron sheet piles from similar environments in the Netherlands showed that a CPL often formed on the interface of the sheet pile and the surrounding sediment (12). This layer was also found on the Gouderak sheet piles. We investigated the geochemical composition and the microbial communities of the CPLs, the surrounding sediment, and the bulk sediment. The metabolic potential of the microorganisms was investigated using Illumina MiSeq sequencing and metagenome

analysis of the same samples, providing a unique insight into the full functional potential of natural CPL communities. This data set was also interrogated to study the microbial community structure using rRNA gene-based phylogeny. The combination of microbial composition data, metabolic potential, and physicochemical parameters enabled us to reconstruct a microbial food web that is likely involved in CPL formation. This study provides insights into the microbiology of corrosion protection processes in freshwater ecosystems and is a follow-up on the microbial-diversity screening study of Kip et al. (12). Our findings could support the development of screening protocols to investigate the current status of iron sheet piles and to decide whether replacement is required.

RESULTS AND DISCUSSION

We studied 4-m-deep sheet piles at a pumping station in Gouderak, the Netherlands, that were removed after 50 years of service. Natural CPLs were observed on the surface of the sheet piles. These deposit layers have the potential to protect iron sheet piles from corrosion, resulting in a longer life span, with corresponding economic and environmental benefits. Therefore, we investigated the community structure and metabolic potential of the natural CPL microbial community, the surrounding sediment more distant to the CPLs, and the top sediment in conjunction with the geochemical composition of the sediments. The microbial community of the deposit layer was studied in detail to unravel the microbial interactions that could potentially lead to the corrosion protection of natural CPLs.

Sediments are rich in organic matter and contain large amounts of calcium and magnesium oxides. Samples were taken in duplicate at the surface for bulk sediment (BS), at 3-m-deep adjacent sediments (AS), and deposit layers (DL) (see Fig. 4). Sediment properties were assessed by X-ray fluorescence and total carbon and sulfur analysis. All sediment samples at 0- and 3-m depths were rich in organic matter, with an average of 75.7%. The AS and DL differed in total C and S content: the sediment attached to the DL contained on average 13.6% C and 0.52% S, whereas AS contained on average 22.8% C and 0.85% S. This indicates a higher carbon turnover around the deposit layers. High percentages of CaO (average, 6.2%; normal soil value, 1%) and MgO (average, 1.0%), the dominant cations in most soils and sediments, indicate that the system was buffered by groundwater fluxes (see Table S1 in the supplemental material) (17, 18). Both cations are important in precipitative layer formation and thus crucial in CPL dynamics. Through changing alkalinity and carbon dioxide concentrations, calcium and magnesium can rapidly form, precipitating mineral oxide and carbonate complexes (19).

Iron corrosion in freshwater ecosystems leads to the formation of iron-oxide complexes and iron carbonates. Under low sulfate conditions, iron oxidation mainly proceeds via the formation of ferrous hydroxide that is transformed into magnetite and hydrogen via the Schikorr reaction:

$$3Fe + 4H_2O \rightarrow Fe_3O_4 + 4H_2 \quad (1)$$

In buffered, calco-carbonated freshwater systems corrosion additionally leads to the formation of a wide variety of minerals, including wustite (FeO), limonite [$FeO(OH) \cdot nH_2O$], and the ferrous carbonates siderite ($FeCO_3$) and chukanovite [$Fe_2(OH)_2CO_3$] (11, 12). The minerals that are formed during biocorrosion in anoxic environments are relatively stable and can protect metal surfaces from further corrosion. Several recent studies focused on biological corrosion inhibition by natural corrosion protective layers (CPLs) (14, 15, 20, 21). Kip et al. detected limonite as candidate enriched mineral in the deposit layer (12). Furthermore, X-ray crystallography analysis indicated wustite, calcite ($CaCO_3$), siderite and chukanovite [$Fe_2(CO_3)(OH)_2$] in two mineral layers on Westerkade sheet piles (12).

16S rRNA gene-based phylogeny indicated the presence of an organic carbon-degrading consortium with enrichment of methanogens in deposit layers. The microbial compositions of BS, AS, and DL were analyzed using 16S rRNA gene reads

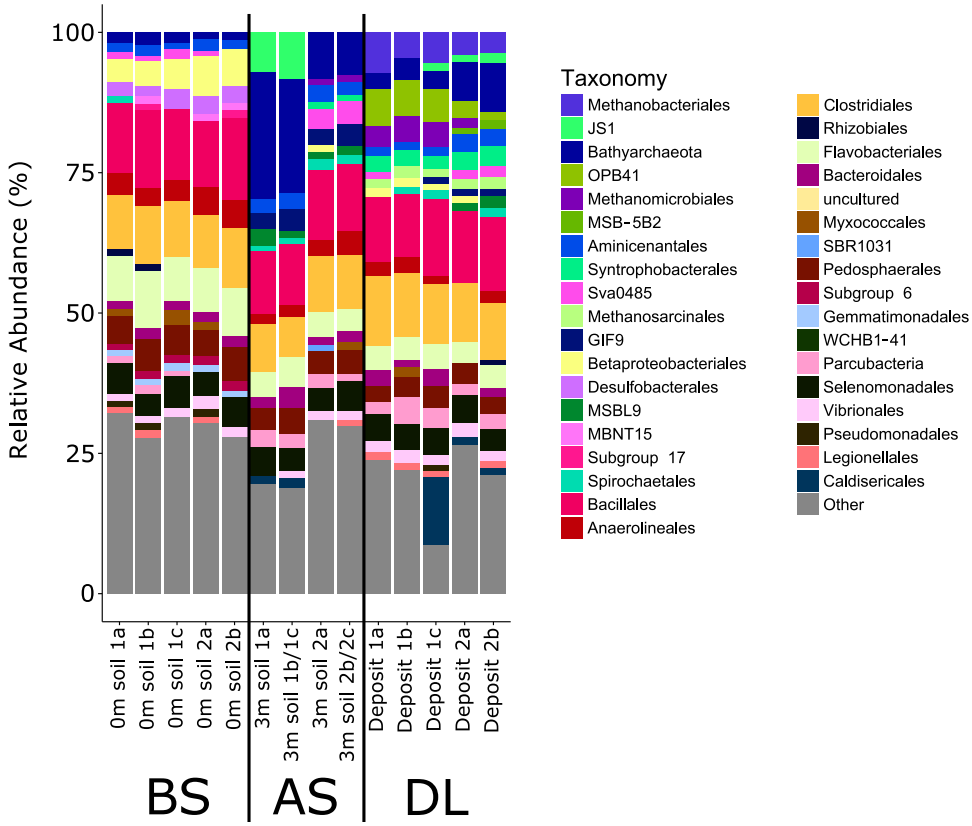

FIG 1 Taxonomic distribution of prokaryotic 16S rRNA gene reads obtained from metagenomic data sets from two bulk sediment samples at the water-sediment interface (BS; 0-m soil samples 1a to c and 2a and b), two surrounding sediment samples (AS; 3-m soil samples 1a, 1b/1c, 2a, and 2b/2c) and two deposit layer samples (DL; samples 1a to c and 2a and b). All taxonomic groups have a relative abundance of ≥1%. "Other" includes all taxonomic groups with a relative abundance of <1%. Taxonomic identification is given up to order level.

derived from 14 metagenomic data sets (Fig. 1; see also Table S2 in the supplemental material) and metagenome-assembled genomes (MAGs) (Table 1; see also Table S3). 16S rRNA gene-based analysis showed equal relative abundances of *Bacillales* (12.4%), *Clostridiales* (10.1%), and *Flavobacteriales* (5.8%) in all locations. *Anaerolineales* (2.9%), *Betaproteobacteriales* (2.4%), and *Bacteroidales* (1.9%) were also omnipresent, but overall relatively less abundant. The *Bathyarchaeota* phylum was more abundant in AS (14.7%), less abundant in DL (5.1%), and least abundant in BS (1.7%). The *Bathyarchaeota* relative abundances strongly differed between AS samples 1 and 2 (21.5 and 8.0%, respectively). This, however, could not be explained by geochemical properties (Table S1). The same pattern was found for the candidate phylum *Atribacteria* (JS1), which showed highest relative abundance in AS sample 1 (7.6%) but showed only low abundance in DL (0.9%) and was not detected in BS.

TABLE 1 Characteristics of the four metagenome-assembled genomes with a completeness of >95%[a]

CheckM taxonomy sister lineage (order)	GC content (%)	Completeness (%)	Redundancy (%)	Strain heterogeneity (%)	Genome size (Mbp)	% coverage of:	
						AS aligned reads	DL aligned reads
Methanobacteriales	32.7	98.9	1.1	100	2.18	0.1	8.7
Coriobacteriales (first MAG)	66.4	96.9	9.0	41.2	2.48	1.5	9.2
Syntrophobacterales	45.7	96.8	1.3	0.0	3.32	0.0	18.1
Coriobacteriales (second MAG)	64.3	95.0	4.7	15.8	2.70	0.1	11.3

[a]Taxonomy sister lineage, GC content, completeness, strain heterogeneity, and genome size were assessed by CheckM. The percent coverage data provide the average aligned read coverage for each sampling location per metagenome-assembled genome (MAG). AS, adjacent soil; DL, deposit layer.

The potential organic matter-degrading community is dominated by *Bacillales*, *Clostridiales*, and *Flavobacteriales*. The average total organic matter content was high (76%) in the metal sheet pile environment due to the presence of peat sediments. Organic matter-degrading guilds are essential for the formation of a methanogenic food web resulting in local changes that can induce CPL formation. *Bacillales* (12%), *Clostridiales* (10%), and *Flavobacteriales* (5.8%) were relatively highly abundant in all samples. These phyla are common members of soil microbial communities (22–24). A study on crude oil contaminated soils indicated their preference for organic carbon-rich environments, which matches our observations in soils with high organic carbon contents (25).

Bacillus spp. are often abundant in soils amended with long-chain alkanes, polysaccharides and polycyclic aromatic hydrocarbons, indicating their potential role in organic matter degradation (26–29). Their high relative abundance observed in our study might be explained by their ability to form spores and the production of antimicrobial compounds and antifungal volatiles (30–32). *Clostridiales* are common anaerobic soil inhabitants that can metabolize a wide variety of complex carbohydrates, including cellulose, leading to the production of ethanol, acetate, CO_2, and H_2, which are essential intermediates in biological organic carbon cycling (23, 33). *Flavobacteriales* are often detected in low-temperature, organic-rich soils and sediments, where they are linked to changes in carbon availability (34, 35). A recent metagenomic study by Rasigraf et al. (36) also found high relative abundances of *Flavobacteriales* in cooccurrence with methanogenic archaea in oligotrophic brackish sediments with large amounts of reactive iron. They were also detected in soil lignolytic communities that are essential for organic compound cycling (24). This supports our observation of *Flavobacteriales* in sediments with plant-based organic matter and reactive iron species.

Anaerolineales (average, 2.9%), *Betaproteobacteriales* (average, 2.4%), and *Bacteroidales* (average, 1.9%) were also detected in all samples. These orders include common soil inhabitants (22, 37, 38). *Betaproteobacteria* (*Syntrophaceae*) and *Bacteroidales* are indicators of soils with higher pH ($>$6.5) and relatively low C:N ratios ($<$12.5) (22). Their occurrence matches with the buffered conditions and high organic matter contents of the sediments in this study. All three orders likely play a role in organic matter degradation, although their exact contributions remain unknown.

***Deltaproteobacteria*, *Bacteroidetes*, and *Bathyarchaeota* potentially have a central role in acetate metabolism.** To study central carbon metabolism, we investigated acetate kinase (*ackA*) and acetyl-coenzyme A synthetase (ACS) gene diversity in DL and AS. Reads were extracted from the quality-processed read data sets. Protein blasts (BLASTP) resulted in the most AckA hits for DL to the *Deltaproteobacterium* bacterium HGW species from a groundwater metagenome study (11.6%) (39), whereas AS reads mostly mapped to the *Bacteroidetes* bacterium RBG from sediment metagenomes (11.0%) (40) (Table S6). For ACS, most DL reads matched to *Methanobacterium* species from coal seam gas formation water (11.0%) (41), *Methanoregulaceae* from sediment metagenomes (5.3%) (42), and *Bathyarchaeota* (4.3%) (40, 43). Of the ACS reads, 19.3% were most identical to HGW species from a groundwater metagenome study (39). For AS, 29.8% of the sequences showed highest identity to *Bathyarchaeota* ACS sequences from sediment metagenomes (40), groundwater metagenomes (43), and hot springs metagenomes (44). A total of 12.6% of the ACS reads mapped to *Chloroflexi* sequences from sediment metagenomes (40) (Table S7). These findings are supported by 16S rRNA gene read analyses that indicate that *Bathyarchaeota* are more abundant and potentially have a central role in organic matter degradation in AS.

Potentially heterotrophic *Bathyarchaeota* and the candidate phylum *Atribacteria* (JS1) were more abundant in adjacent sediment. *Bathyarchaeota* are generally described as heterotrophic microorganisms with the genomic potential to metabolize cellulose, lignin, and aromatic compounds (45–47). They were previously detected in methanogenic communities, where they can have close spatial associations with *Methanomicrobia* (48, 49). Interestingly, a study by Xiang et al. (48) found a significant correlation between occurrence of *Bathyarchaeota* and *Methanomicrobia*, indicating a

potential syntrophic association between the two phyla (48). Here, we also observed the cooccurrence of *Methanomicrobiales* (2.9% in DL and 1.1% in AS [sample 2]) and *Bathyarchaeota* (5.1% in DL and 14.7% in AS). Their role in methane cycling communities, however, still needs to be elucidated.

Candidate phylum *Atribacteria* (JS1) is found globally in anoxic marine sediments, deep biospheres, and petroleum reservoirs (50–52). Genomic data mining indicates that candidate phylum JS1 species most probably have heterotrophic fermenting and syntrophic lifestyles (52). A recent study by Glass et al. (53) found candidate JS1 bacteria with low temperature and salinity adaptation in subseafloor gas hydrates. This indicates a wide tolerance range and a preference of JS1 for methane-rich environments. Network analyses support the cooccurrence of candidate phylum JS1 with H_2 and formate-scavenging methanogens and propionate metabolizers (54). They are less abundant in the deposit layer communities but might play a role in the nutrient cycling of deeper sediments.

***Coriobacteriales*, *Syntrophobacterales*, and the actinobacterial order OPB41 are key members of the deposit layer microbial communities.** *De novo* assembly and consensus binning resulted in a total of 16 MAGs with an estimated genome completeness >50% (data not shown). A total of 81% of the reads were aligned to MAGs. We obtained four nearly complete MAGs (>95% completeness) that were all highly enriched in DL but showed low abundance in AS (average aligned read coverage of the MAGs, <1.5%) and BS (average aligned read coverage of the MAGs, <0.02%) (Table 1). Initial taxonomic classification by CheckM indicated two *Coriobacteriales* MAGs, one *Syntrophobacterales* MAG, and one *Methanobacteriales* MAG that together contained 47% of the mapped reads of the deposit layer microbial community. These four MAGs were analyzed for their potential role in nutrient cycling and natural CPL formation.

The two highly complete *Coriobacteriales* MAGs contained 20.5% of all mapped DL reads. Although *Coriobacteriales* were not detected with the 16S rRNA gene survey, the large number of reads aligning to the MAGs indicates their potentially important role in DL. *Coriobacteriales* are an order within the *Actinobacteria* that are known for their important role in nutrient cycling of soils (55, 56). *Actinobacteria* have a central role in decomposition of dead organic matter, including lignin solubilization (55). A study by Gupta et al. (57) on acidic mine drainage soils indicated that *Coriobacteriaceae* can perform extracellular electron transport probably through use of *c*-type cytochromes and monomethylmenaquinone-6, its major respiratory quinone, as shown by growth on anodes in fuel cells (58, 59). The production of menaquinone-6 homologues of vitamin K_2 seems to be a common attribute of the *Coriobacteriaceae* (59). The potential for extracellular electron transport can be an important feature when iron is abundantly present.

16S/23S rRNA genes were only obtained from one of the two *Coriobacteriaceae* MAGs. The 16S rRNA gene (1,509 nucleotides [nt]) was most identical (97% nt identity) to an uncultured actinobacterium clone, EMTBiocatB-13, from the biocathode of a thermophilic fuel cell catalyzing electromethanogenesis (KM819482.1) (60). Regarding cultivated bacteria, it had the highest identity to *Raoultibacter* sp. strain Marseille-P8396 (90% nt identity). The 23S rRNA gene (2,633 nt) was most identical (85% nt identity) to *Gordonibacter massiliensis* Marseille-P2775 isolated from a human fecal sample (61). These findings indicate that the two environmental *Coriobacteriales* MAGs are distantly related to *Coriobacteriales* isolated from human microbiomes. 30S and 50S rRNA analyses showed highest identity of the first *Coriobacteriales* MAG (89% average amino acid [aa] identity) to *Actinobacteria* bacterium 66_15 isolated from a terrestrial environment in the Schrader Bluff formation on the Alaska North Slope (taxonomy ID 1635289) (62). The second *Coriobacteriales* MAG was most identical (90% aa identity) to *Actinobacteria* bacterium HGW-Actinobacteria-1 and Actinobacteria-6, which were detected in deep terrestrial subsurface sediments that were actively transforming H_2 and metals (39) (see Tables S10, S11, S14, and S15 in the supplemental material).

Both MAGs contained the Wood-Ljungdahl pathway for carbon fixation (Tables S11 and S15). From the second MAG, two ACS genes were identified with the highest

identities to the *Actinobacteria* bacterium HGW-Actinobacteria-6 (94 and 88% aa identities) (39) (Table S15). The most closely related ACS sequences of cultivated representatives belonged to *Thermodesulfovibrio thiophilus* and *T. aggregans* (67 and 65% aa identities, respectively).

The functional roles of environmental *Coriobacteriales* species are mostly unknown (63). *Desulfobacterales* and *Coriobacteriales* were detected as main benzene degraders in a DNA-stable isotope study with [^{13}C]benzene (64). Comparative analyses of ^{12}C and ^{13}C-labeled samples further indicated the enrichment of *Methanosarcinales* (64). Here, we observed two *Coriobacteriales* MAGs in cooccurrence with methanogens, supporting a central role in organic matter-degrading methanogenic cultures.

Syntrophobacterales were relatively more abundant in DL, with an average 3.0% abundance compared to 1.3% in AS sample 2. Metagenomic binning resulted in one nearly complete *Syntrophobacterales* MAG containing 18.1% of total mapped DL reads and no reads from AS. The partial 16S and 23S rRNA genes were retrieved (1,564 and 2,016 nt) with the highest identity for the 16S rRNA gene to *Syntrophaceae*-related clones (96%) and *Syntrophus aciditrophicus* strain SB (93%), which was also the best hit for the 23S rRNA gene (65). The 16S rRNA gene was most identical to sequences from a methanogenic hexadecane-degrading culture enriched in *Syntrophaceae* (66). For additional 30S and 50S ribosomal subunit and functional gene analyses, see Tables S12 and S13 in the supplemental material. Some *Syntrophobacterales* species can reduce sulfate but most syntrophically oxidize fatty acids and alcohols to acetate, H_2, and CO_2 (67). Their metabolism could thus fuel methanogenic archaea. Cooccurrence of *Syntrophobacterales* and both acetoclastic and hydrogenotrophic methanogens is common in soils and lake sediments (68, 69). A study by Lueders et al. (70) showed that *Syntrophobacterales* syntrophically oxidized propionate in cooccurrence with *Methanobacterium* and *Methanosarcina* species. These findings indicate that *Syntrophobacterales* potentially have key roles in organic compound conversion to methanogenic substrates in the organic-rich sediments surrounding the metal sheet piles.

The actinobacterial order OPB41 was enriched in the deposit layers and had an average relative abundance of 4.7%. These organisms cooccur with *Methanobacteriaceae* in coal beds (71, 72). In coal-bearing strata of the Cherokee Basin, USA, the actinobacterial order OPB41 cooccurred with *Clostridia*, *Deltaproteobacteria*, and an archaeal community that was dominated (>80% relative abundance) by methanogens (*Methanococcales*, *Methanobacteriales*, *Methanomicrobiales*, and *Methanosarcinales*) (72). Here, we also found cooccurrence of OPB41 with both hydrogenotrophic and acetoclastic methanogens.

The methanogenic community is enriched 18-fold in deposit layers compared to the surrounding sediment. More than 18% of the reads were aligned to methanogen MAGs with more than 50% genome completeness. The methanogenic community consisted of hydrogenotrophic *Methanobacteriales* (4.9%), *Methanomicrobiales* (2.9%), and versatile *Methanosarcinales* (1.8%). Methanogens were enriched 18-fold in DL compared to AS in which only *Methanomicrobiales* were detected in AS sample 2 (1.1%). Metagenome binning resulted in MAGs from the orders *Methanobacteriales* (three MAGS obtained from DL with 8.7, 3.2, and 2.7% of total mapped reads), *Methanomicrobiales* (one MAG with 2.9% of total mapped deposit reads), and *Methanosarcinales* (one MAG with 0.9% of mapped DL reads) (Table 1; see also Table S4 in the supplemental material). The diversity of the methanogenic community supports a central role of H_2 and acetate transfer. Acetate is essential for the growth of acetoclastic methanogens, but it is also important in supporting the growth of hydrogenotrophic *Methanomicrobiaceae* (73). 16S rRNA gene reads from the metagenomic data sets were extracted per phylogenetic group and assembled *de novo* for deeper phylogenetic analysis. This resulted in two *Methanobacterium* 16S rRNA gene contigs. Contig 1 (685 bp, 49× coverage) was most identical (99%) to the hydrogenotrophic methanogen *Methanobacterium palustre* strain F (NR_041713.1) isolated from a mesophilic corn-fed on-farm biogas plant (74). Contig 2 (839 bp, 29× coverage) was most identical

(98%) to *Methanobacterium kanagiense* strain 169 (NR_112749.1) isolated from an anaerobic propionate-oxidizing enrichment culture from a rice paddy field soil (75).

To further investigate methanogen diversity of the deposit layers, the diversity of the methyl-coenzyme M reductase alpha subunit, *mcrA*, was investigated. *mcrA* reads were extracted from the raw read data sets, and their analysis generally supported the high diversity of the methanogenic community. Of the translated *mcrA* reads, 22.7% were most identical to that of *Methanobacterium* sp. strain Maddingley MBC34 (EKQ53862) isolated from a coal seam gas formation water sample (41) (Table S5). Of the translated reads, 6.2% gave best hits to sequences from uncultured archaeon sequences from Lake Pavin 90-m-depth samples which were dominated by sequences linked to hydrogenotrophic methanogenic archaea (76) (Table S5). There were no hits to McrA sequences of anaerobic methanotrophic archaea.

The methanogenic community of deposit layers was dominated by a *Methanobacteriales* MAG related to a *Methanobacterium* sp. Due to its high abundance in the deposit layers (8.7% of mapped reads) and completeness of the MAG (98.9%), the first *Methanobacteriales* MAG was investigated more closely. Phylogenetic analysis based on a partial 16S rRNA gene sequence (925 nt) showed the highest identity to *Methanobacterium oryzae* strain FPi (NR_028171.1, 97%) isolated from a rice paddy field soil (77, 78). The 23S rRNA gene (2,970 nt) was most identical to the hydrogenotrophic methanogen *Methanobacterium palustre* strain F (KF882001.1, 97%), which was also detected in the 16S rRNA gene *de novo* assembly approach. *M. palustre* was isolated from a peat bog (79). Both *M. oryzae* and *M. palustre* were isolated from organic carbon-rich freshwater environments. For further identification, a total of 55 30S and 50S ribosomal proteins were identified. Forty-nine proteins gave best hits to multispecies *Methanobacterium* sequences (89% average aa identity); at the species level, the average identity was 84%, with most hits to *Methanobacterium congolense* (35% of proteins, 83% aa identity), *Methanobacterium* sp. strain SMA-27 (16% of proteins, 84% aa identity), and *Methanobacterium formicicum* (11% of proteins, 85% aa identity) (Table S8). These findings and the high strain heterogeneity observed by CheckM indicate the presence of multiple novel *Methanobacteriales* strains in DL. For detailed functional gene analyses, see Table S9.

Elemental iron is a potential substrate for acetogenic and methanogenic communities. Methanogens were relatively more abundant and more diverse at the iron sheet piles than in the surrounding and top sediment. The hydrogen partial pressure does not seem to be the driving factor of methanogen community composition since the more-abundant *Methanobacterium* spp. have lower affinity for H_2 than the less-abundant *Methanomicrobiales* (80). Since sulfate is not relevant at the study site, significant competition with sulfate-reducing hydrogen oxidizers is unlikely (81). This suggests that there might be a central role for elemental iron in structuring the microbial community in CPLs.

The ability to accept electrons via direct interspecies electron transfer (DIET) can be an important factor in shaping the methanogenic community. *Methanosarcinales* possess *c*-type cytochromes that play a role in DIET, as shown for cocultures with *Geobacter metallireducens* (82). A recent study by Yee et al. (83) showed the ability of *Methanosarcina* species to directly accept electrons from insoluble electron donors, including conductive particles and biocathodes that show similarities to the metal sheet piles in our study. A study by Jaramillo et al. (84) observed a competition of *Methanosarcina* species with acetogens in nonsulfidic environments. The study's observations of higher methanogenesis rates without a mixed community that includes *Clostridiales* indicated a competition to obtain electrons from elemental iron. This finding supports a central role for elemental iron in structuring the community.

Methanomicrobiales and *Methanobacteriales* do not possess *c*-type cytochromes (85). However, the archaellum of *Methanobacteriales* species *Methanospirillum hungatei*, which is structurally related to the type IV pilus, is electrically conductive (86). Similar observations have been well described for *Methanococcus* species (87). In addition, iron minerals such as magnetite (Fe_3O_4) and, to a lesser extent, limonite and wustite were

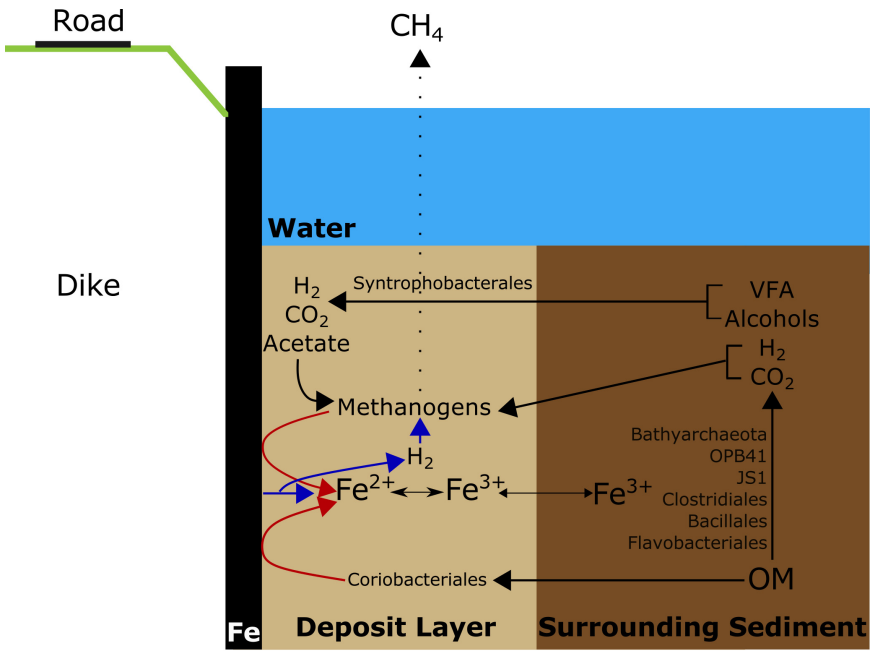

FIG 2 Scheme illustrating the potential microbial food web of the deposit layer and the surrounding iron sheet pile (indicated by "Fe") and organic-rich sediment. The microbial community of the surrounding sediment has the capacity to degrade organic matter (OM) to volatile fatty acids (VFA), alcohols, H_2, and CO_2. *Syntrophobacterales* can syntrophically oxidize VFA and alcohols to H_2, CO_2, and acetate. Methanogens can use substrates produced by the bacterial community and potentially directly obtain electrons from iron oxidation. Black arrows indicate microbial conversions, red arrows indicate redox reactions that involve extracellular electron transfer, and blue arrows indicate abiotic iron oxidation.

observed in natural CPLs by Kip et al. (12). These can compensate for the lack of pilin-associated *c*-type cytochromes, as shown for *Geobacter sulfurreducens* (88). The methanogen diversity might be further explained by the absence of mixing and disturbances, which could result in the formation of small niches (89). At low temperatures, hydrogenotrophic methanogens with higher affinity for H_2 than homoacetogens can win the competition in syntrophic reactions of fatty acid decomposition (90). This could explain the relatively high metabolic complexity and diversity of the methanogenic archaea in DL.

Role of iron under anoxic conditions. The microbial community in DL is distinctive from that in AS. It is therefore tempting to speculate that the microbial community is responsible for the formation of the CPLs. Several methanogenic archaeal MAGs were enriched in the metagenomes of DL. Genomic metabolic potential analysis of the MAGs unique to DL indicated that they form an anaerobic food chain degrading organic matter under methanogenic conditions (Fig. 2). The background community was typical for organic-rich sediments and showed similarities between AS and DL. The sheet piles are initially placed in a mildly corrosive environment, potentially facilitating growth of methanogenic archaea. Closely related methanogens were shown to use elemental iron as a direct electron source (3). Dinh et al. (3) isolated a *Methanobacterium*-like species under low-sulfate conditions with supplementation of elemental iron. Interestingly, this species grew faster when iron was provided, and strictly hydrogenotrophic growth was slow and only obtained at pH >7.5. This growth strategy could also be facilitated in the initial phase of iron sheet pile placement in the anoxic methanogenic sediments. Some hydrogenotrophic methanogens can also directly reduce ferrihydrite, whereas some acetoclastic methanogens can switch between methanogenesis and iron reduction (91, 113–115).

In addition, in a study on anaerobic benzene-oxidizing, iron-reducing cultures, Kunapuli et al. (92) hypothesized that electrons from benzene degradation can be directly transferred to ferric iron or shared between community members, including

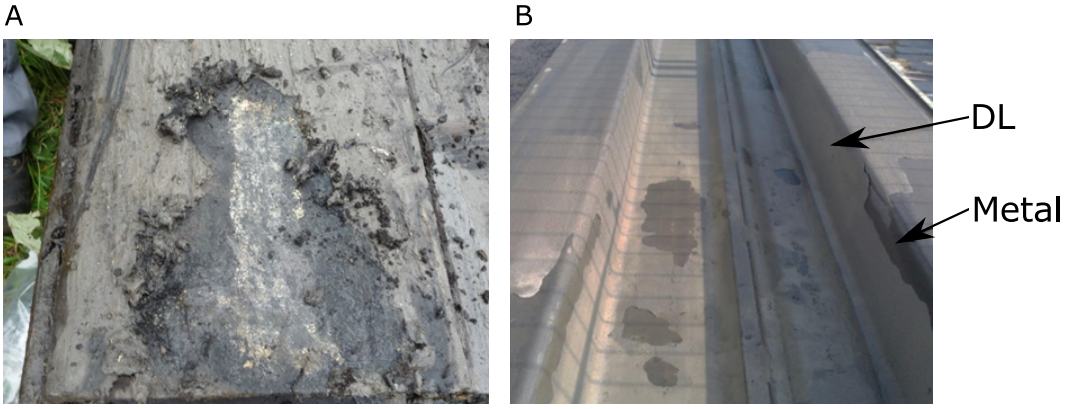

FIG 3 (A) Picture of sediment and deposit layers visible on a sheet pile sampled at the pumping station of Gouderak. (B) Picture of deposit layer at Rotterdam Harbor sheet piles after careful removal of sediment layers. Pictures were taken by N.K.

methanogens (92). The interactions between methanogenesis and iron reduction are highly complex, and there are strong indications that both processes can occur simultaneously (93–95).

Besides biotic processes, iron dissolves slowly and forms H_2 with protons (H^+) from water ($Fe + 2H_2O \leftrightarrow Fe^{2+} + H_2 + 2OH^-$; $E0' = -0.03$ V). Although this is a slow process, it can be accelerated by microbial hydrogen consumption, such as hydrogenotrophic methanogenesis. This could be relevant in shaping the initial microbial community over the life span of iron sheet piles.

A possible reason for the subsequent formation of the CPLs could be the change of pH elicited by the activity of the ferrotrophic/hydrogenotrophic methanogens. In contrast, the degradation of complex organic compounds under lower methanogenic activity leads to an equilibrium at more acidic pH that is less optimal for mineral precipitation (96). At the iron sheet piles, the presence of methanogens leads to the consumption of CO_2 that is in equilibrium with carbonate and will result in a local pH increase at the iron sheet pile surface. Because of calcium- and magnesium-rich groundwater fluxes, a locally increased pH can facilitate the precipitation of iron, calcium, and magnesium minerals.

This deposit layer additionally protects the iron sheet pile from corrosion by buffering the sheet pile surface from direct acidification. Since the microbial community in and surrounding the DL stays active, the CPL can be maintained (see Fig. 4). This significantly increases the life span of iron sheet piles, reducing safety risks and the economic costs of replacement. Our current understanding of natural CPLs, however, remains limited. More research confirming the role and metabolic activity of key players in CPL formation in freshwater ecosystems is therefore highly needed.

MATERIALS AND METHODS

Sample collection and physicochemical analysis. The pumping station of Gouderak (Zuid-Holland, the Netherlands, 51°59′1.233″N, 4°40′20.654″E) was constructed in 1866 and is used for land drainage. It removes water from the Stolwijksche Boezem into the river Hollandse IJssel. Sheet piles that were installed 50 years ago were pulled out of the ground on 31 May 2012 and 6 June 2012 for renovation work on the pumping station and its surroundings. The sheet piles were 5 to 6 m long and driven up to 4 m into the sediment. The part exposed to the atmosphere was occasionally submerged at high tide. The belowground part of the sheet pile did not show any signs of corrosion. However, different deposit layers were visible at various depths (Fig. 3). Samples were taken from the sheet pile directly after extraction.

Sediment samples were taken from the top layer (bulk sediment [BS]) and at three meters depth surrounding the sheet pile, at most 5 cm from the sheet pile (adjacent sediment [AS]) (Fig. 4). Deposit layers were sampled as aseptically as possible and, where possible, layers were scraped off. Samples taken on 31 May were immediately stored under anoxic conditions, transported on ice, and stored at −20°C. Samples from 6 June were stored at −20°C after transport. See Table S3 in the supplemental material for additional sample information.

Physicochemical parameters (total C and S, SiO_2, AlO_3, TiO_2, Fe_2O_3, MnO, CaO, MgO, Na_2O, K_2O, P_2O_5, soil organic matter, Cr, Ni, Sr, Ba, Zr, Si, Al, Ti, Fe, Mn, Ca, Mg, Na, K, and P) were analyzed by Deltares

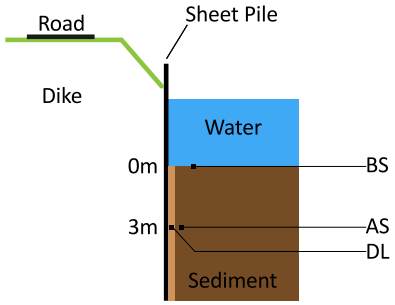

FIG 4 Overview of the sheet pile sampling procedure. The sheet pile is located at the boundary between the dike and the canal. The bulk sediment (BS) sample was taken at the top of the sediment layer; the surrounding/adjacent sediment (AS) and the deposit layers (DL) were sampled at 3 m below the sediment water interface. The AS samples were taken 1 to 5 cm away from the DL.

(Utrecht, the Netherlands) using X-ray fluorescence. Total C and S were determined by flash combustion and CO_2 analysis with a LECO SC-632 IR detector. Additional parameters were determined for the sites Giessenburg and Nieuwlekkerland (see Kip et al. [12] for extensive details).

Molecular analysis. (i) DNA extraction and sequencing. DNA was extracted from 0.25 to 0.3 g of (ground) sample using a PowerSoil DNA isolation kit (Qiagen, Venlo, the Netherlands) according to the manufacturer's protocol, with 10-min bead beating at 30 Hz instead of vortexing. The DNA concentration of each sample was measured using an ND-1000 spectrophotometer (Thermo Fisher Scientific, Waltham, MA). Sequencing libraries were constructed using a TruSeq Nano kit (Illumina, Inc., San Diego, CA) and sequenced using an MiSeq desktop sequencer (Illumina; Macrogen, Inc., Seoul, South Korea). Samples with a low DNA yield were excluded due to technical restrictions.

(ii) Metagenome analysis. Quality-trimming, sequencing adapter removal and contaminant filtering of Illumina paired-end sequencing reads were performed using BBDuk (BBTOOLS v37.76) (97). Processed reads for selected samples were coassembled *de novo* using metaSPAdes v3.11.1 (98) at default settings. metaSPAdes iteratively assembled the metagenome using k-mers of lengths 21, 33, 55, 77, 99, and 127. Reads were mapped back to the assembled metagenome for each sample separately using Burrows-Wheeler Aligner 0.7.17 (BWA) (99), employing the "mem" algorithm. The sequence mapping files were processed using SAMtools 1.6 (100). Metagenome binning was performed for contigs greater than 1,500 bp. To optimize binning results, five binning algorithms were used: BinSanity v0.2.6.1 (101), COCACOLA (102), CONCOCT (103), MaxBin 2.0 2.2.4 (104), and MetaBAT 2 2.12.1 (105). The five bin sets were supplied to DAS Tool 1.0 (106) for consensus binning to obtain the final bins. The quality of the generated genome bins was assessed through a single-copy marker gene analysis using CheckM 1.0.7 (107). Genomes were annotated with Prokka 1.12 (108) using the NCBI Reference Sequence Database (RefSeq), release 85 (109). The predicted coding sequences were submitted to the KEGG Automatic Annotation Server (KAAS [last update, 3 April 2015]) (110) for pathway analyses using the 40 most closely related organisms available in the KEGG Organisms Database as a reference (https://www.genome.jp/kegg/catalog/org_list.html; last update, 18 December 2018 [see the supplemental material for the KAAS analysis reference genomes]). Genome annotations were examined using the Artemis genome browser, release 16.0.0 (111). For 16S rRNA gene analysis, unprocessed Illumina MiSeq reads were mapped against the SILVA SSU nonredundant database version 132 and *de novo* assembled as described in in 't Zandt et al. (112). In short, sequencing reads were assembled *de novo* using stringent similarity and length fraction parameters of 0.95 to obtain nearly complete 16S rRNA gene sequences. Specific marker protein sequences for methane cycling (methyl-coenzyme M reductase [McrA], particulate methane monooxygenase [PmoA], and soluble methane monooxygenase [MmoX]) and acetate metabolism (acetate kinase [AckA], ACS, and carbon monoxide dehydrogenase [CODH]) were selected and downloaded from the NCBI (see the supplemental material for NCBI database generation). Analysis of trimmed reads was performed using the BLASTX (BLAST 2.2.25+) algorithm with an E value of 0.0001, extracting first hits as a target sequence. Output sequences were manually checked and filtered on bitscore to obtain true hits. For McrA, the bitscore was set to ≥100, for PmoA and MmoX no true sequences were obtained, for AckA the bitscore was set to ≥80, for ACS the bitscore was set to ≥80, and for CODH no true target hits were obtained. For each draft genome bin the selected genes were also obtained. For the final species identification, the bitscore-filtered reads were blasted against the NCBI nonredundant protein database (13 December 2018) using CLC Genomics Workbench 11 with custom settings Expect 10.0, Word size 3, Matrix BLOSUM62 and gap costs Existence 11, Extension 1. To extract reads that matched the 16S rRNA gene used for taxonomic classification, all reads were mapped against the SILVA SSU 132 data set using CLC Genomics Workbench v11. Length and similarity fraction were set to 50 and 70%, respectively, and values for mismatch, insertion and deletion cost to 2, 3 and 3, resulting in a total of 63,478 mapped reads (0.25% of total). The extracted 16S rRNA gene reads were also used for *de novo* assembly. 16S rRNA gene contigs were assessed using nucleotide BLAST against the NCBI GenBank as described by in 't Zandt et al. (112).

Data availability. MiSeq sequencing data were deposited in the European Nucleotide Archive under accession number ERP008629.

SUPPLEMENTAL MATERIAL

Supplemental material for this article may be found at https://doi.org/10.1128/AEM.01369-19.

SUPPLEMENTAL FILE 1, PDF file, 0.8 MB.

ACKNOWLEDGMENTS

All authors designed and M.H.I.T.Z. and N.K. performed the experiments. N.K. and S.J. collected the data. M.H.I.T.Z., J.F., and N.K. analyzed the data. M.H.I.T.Z. and N.K. wrote the paper with contributions from S.J., J.A.V.V., M.S.M.J., and C.U.W.

M.H.I.T.Z., J.F., C.U.W., and M.S.M.J. were supported by the Nederlandse Organisatie voor Wetenschappelijk Onderzoek through the Soehngen Institute of Anaerobic Microbiology Gravitation Grant 024.002.002 and the Netherlands Earth System Science Center Gravitation Grant 024.002.001. M.S.M.J. was supported by the European Research Council Advanced Grant Ecology of Anaerobic Methane Oxidizing Microbes 339880. N.K., J.A.V.V., and S.J. were supported by the Dutch Technology Foundation STW (currently the NWO Domain Applied and Engineering Sciences [AES]), which is part of the Netherlands Organization for Scientific Research (NWO), and which is partly funded by the Ministry of Economic Affairs grant number 11333.

This is publication number 6802 of the NIOO-KNAW, Netherlands Institute of Ecology. The funding agencies had no role in study design, data collection and interpretation, or the decision to submit the work for publication.

REFERENCES

1. Beech IB, Sztyler M, Gaylarde CC, Smith WL, Sunner J. 2014. Biofilms and biocorrosion, p 33–56. *In* Liengen T, Féron D, Basségny R, Beech IB (ed), Understanding biocorrosion. Woodhead Publishing, Sawston, UK.
2. Flemming HC. 1995. Eating away at the infrastructure: the heavy cost of microbial corrosion. Water Qual Int 4:16–19.
3. Dinh HT, Kuever J, Mussmann M, Hassel AW, Stratmann M, Widdel F. 2004. Iron corrosion by novel anaerobic microorganisms. Nature 427:829–832. https://doi.org/10.1038/nature02321.
4. Beech IB, Gaylarde CC. 1991. Microbial polysaccharides and corrosion. Int Biodeterior 27:95–107. https://doi.org/10.1016/0265-3036(91)90002-9.
5. Rossum JR. 1983. Fundamentals of metallic corrosion in fresh water. CiteSeerX 1983:1–18.
6. Enning D, Venzlaff H, Garrelfs J, Dinh HT, Meyer V, Mayrhofer K, Hassel AW, Stratmann M, Widdel F. 2012. Marine sulfate-reducing bacteria cause serious corrosion of iron under electroconductive biogenic mineral crust. Environ Microbiol 14:1772–1787. https://doi.org/10.1111/j.1462-2920.2012.02778.x.
7. AlAbbas FM, Bhola SM, Spear JR, Olson DL, Mishra B. 2013. The shielding effect of wild type iron reducing bacterial flora on the corrosion of linepipe steel. Eng Fail Anal 33:222–235. https://doi.org/10.1016/j.engfailanal.2013.05.020.
8. Rao TS, Sairam TN, Viswanathan B, Nair K. 2000. Carbon steel corrosion by iron oxidising and sulphate reducing bacteria in a freshwater cooling system. Corros Sci 42:1417–1431. https://doi.org/10.1016/S0010-938X(99)00141-9.
9. Ilhan-Sungur E, Cansever N, Cotuk A. 2007. Microbial corrosion of galvanized steel by a freshwater strain of sulphate reducing bacteria (*Desulfovibrio* sp.). Corros Sci 49:1097–1109. https://doi.org/10.1016/j.corsci.2006.05.050.
10. Rao TS, Kora AJ, Anupkumar B, Narasimhan SV, Feser R. 2005. Pitting corrosion of titanium by a freshwater strain of sulphate reducing bacteria (*Desulfovibrio vulgaris*). Corros Sci 47:1071–1084. https://doi.org/10.1016/j.corsci.2004.07.025.
11. Saheb M, Neff D, Dillmann P, Descostes M, Matthiesen H. 2013. Long-term anoxic corrosion of iron, p 260–284. *In* Dillmann P, Watkinson D, Angelini E, Adriaens A (ed), Corrosion and conservation of cultural heritage metallic artefacts. Woodhead Publishing, Sawston, UK.
12. Kip N, Jansen S, Leite MFA, de Hollander M, Afanasyev M, Kuramae EE, van Veen JA. 2017. Methanogens predominate in natural corrosion protective layers on metal sheet piles. Sci Rep 7:1–11. https://doi.org/10.1038/s41598-017-11244-7.
13. Herrera LK, Videla HA. 2009. Role of iron-reducing bacteria in corrosion and protection of carbon steel. Int Biodeterior Biodegradation 63:891–895. https://doi.org/10.1016/j.ibiod.2009.06.003.
14. Videla HA, Herrera LK. 2009. Understanding microbial inhibition of corrosion: a comprehensive overview. Int Biodeterior Biodegradation 63:896–900. https://doi.org/10.1016/j.ibiod.2009.02.002.
15. Zuo R. 2007. Biofilms: strategies for metal corrosion inhibition employing microorganisms. Appl Microbiol Biotechnol 76:1245–1253. https://doi.org/10.1007/s00253-007-1130-6.
16. Dean JF, Middelburg JJ, Röckmann T, Aerts R, Blauw LG, Egger M, Jetten MSM, de Jong AEE, Meisel OH, Rasigraf O, Slomp CP, in 't Zandt MH, Dolman AJ. 2018. Methane feedbacks to the global climate system in a warmer world. Rev Geophys 56:207–250. https://doi.org/10.1002/2017RG000559.
17. Donahue RL, Miller RW, Shickluna JC. 1977. Soils: an introduction to soils and plant growth, 4th ed, p 135–136. Prentice-Hall, Upper Saddle River, NJ.
18. Roy RN, Finck A, Blair GJ, Tandon H. 2006. Plant nutrition for food security: a guide for integrated nutrient management, p 43–90. Food and Agriculture Organization of the United Nations, Rome, Italy.
19. Irving L. 1926. The precipitation of calcium and magnesium from sea water. J Mar Biol Assoc 14:441–446. https://doi.org/10.1017/S002531540000792X.
20. Kip N, van Veen JA. 2015. The dual role of microbes in corrosion. ISME J 9:542–551. https://doi.org/10.1038/ismej.2014.169.
21. Esnault L, Jullien M, Mustin C, Bildstein O, Libert M. 2011. Metallic corrosion processes reactivation sustained by iron-reducing bacteria: implication on long-term stability of protective layers. Phys Chem Earth A/B/C 36:1624–1629. https://doi.org/10.1016/j.pce.2011.10.018.
22. Kuramae EE, Yergeau E, Wong LC, Pijl AS, Veen JA, Kowalchuk GA. 2012. Soil characteristics more strongly influence soil bacterial communities than land-use type. FEMS Microbiol Ecol 79:12–24. https://doi.org/10.1111/j.1574-6941.2011.01192.x.
23. Tracy BP, Jones SW, Fast AG, Indurthi DC, Papoutsakis ET. 2012. Clostridia: the importance of their exceptional substrate and metabolite diversity for biofuel and biorefinery applications. Curr Opin Biotechnol 23:364–381. https://doi.org/10.1016/j.copbio.2011.10.008.
24. Pold G, Melillo JM, DeAngelis KM. 2015. Two decades of warming increases diversity of a potentially lignolytic bacterial community. Front Microbiol 6:480. https://doi.org/10.3389/fmicb.2015.00480.
25. Abbasian F, Lockington R, Megharaj M, Naidu R. 2016. The biodiversity changes in the microbial population of soils contaminated with crude

oil. Curr Microbiol 72:663–670. https://doi.org/10.1007/s00284-016-1001-4.
26. Kim ES, Lee HJ, Bang W-G, Choi I-G, Kim KH. 2009. Functional characterization of a bacterial expansin from *Bacillus subtilis* for enhanced enzymatic hydrolysis of cellulose. Biotechnol Bioeng 102:1342–1353. https://doi.org/10.1002/bit.22193.
27. Ghazali FM, Rahman R, Salleh AB, Basri M. 2004. Biodegradation of hydrocarbons in soil by microbial consortium. Int Biodeterior Biodegradation 54:61–67. https://doi.org/10.1016/j.ibiod.2004.02.002.
28. Cerniglia CE. 1993. Biodegradation of polycyclic aromatic hydrocarbons. Curr Opin Biotechnol 4:331–338. https://doi.org/10.1016/0958-1669(93)90104-5.
29. Samanta SK, Singh OV, Jain RK. 2002. Polycyclic aromatic hydrocarbons: environmental pollution and bioremediation. Trends Biotechnol 20:243–248. https://doi.org/10.1016/S0167-7799(02)01943-1.
30. Yilmaz M, Soran H, Beyatli Y. 2006. Antimicrobial activities of some *Bacillus* spp. strains isolated from the soil. Microbiol Res 161:127–131. https://doi.org/10.1016/j.micres.2005.07.001.
31. Siala A, Hill IR, Gray T. 1974. Populations of spore-forming bacteria in an acid forest soil, with special reference to *Bacillus subtilis*. J Gen Microbiol 81:183–190. https://doi.org/10.1099/00221287-81-1-183.
32. Zou C-S, Mo M-H, Gu Y-Q, Zhou J-P, Zhang K-Q. 2007. Possible contributions of volatile-producing bacteria to soil fungistasis. Soil Biol Biochem 39:2371–2379. https://doi.org/10.1016/j.soilbio.2007.04.009.
33. Warnick TA, Methé BA, Leschine SB. 2002. *Clostridium phytofermentans* sp. nov., a cellulolytic mesophile from forest soil. Int J Syst Evol Microbiol 52:1155–1160. https://doi.org/10.1099/00207713-52-4-1155.
34. Campbell BJ, Polson SW, Hanson TE, Mack MC, Schuur E. 2010. The effect of nutrient deposition on bacterial communities in Arctic tundra soil. Environ Microbiol 12:1842–1854. https://doi.org/10.1111/j.1462-2920.2010.02189.x.
35. Aislabie JM, Chhour K-L, Saul DJ, Miyauchi S, Ayton J, Paetzold RF, Balks MR. 2006. Dominant bacteria in soils of Marble Point and Wright Valley, Victoria Land, Antarctica. Soil Biol Biochem 38:3041–3056. https://doi.org/10.1016/j.soilbio.2006.02.018.
36. Rasigraf O, van Helmond N, Frank J, Lenstra WK, Egger M, Slomp CP, Jetten M. 2019. Metagenomic analysis reveals large potential for carbon, nitrogen and sulfur cycling in coastal methanic sediments of the Bothnian Sea. bioRxiv https://doi.org/10.1101/553131.
37. Yun J, Zhuang G, Ma A, Guo H, Wang Y, Zhang H. 2012. Community structure, abundance, and activity of methanotrophs in the Zoige Wetland of the Tibetan Plateau. Microb Ecol 63:835–843. https://doi.org/10.1007/s00248-011-9981-x.
38. Chemerys A, Pelletier E, Cruaud C, Martin F, Violet F, Jouanneau Y. 2014. Characterization of novel polycyclic aromatic hydrocarbon dioxygenases from the bacterial metagenomic DNA of a contaminated soil. Appl Environ Microbiol 80:6591–6600. https://doi.org/10.1128/AEM.01883-14.
39. Hernsdorf AW, Amano Y, Miyakawa K, Ise K, Suzuki Y, Anantharaman K, Probst A, Burstein D, Thomas BC, Banfield JF. 2017. Potential for microbial H_2 and metal transformations associated with novel bacteria and archaea in deep terrestrial subsurface sediments. ISME J 11:1915–1929. https://doi.org/10.1038/ismej.2017.39.
40. Anantharaman K, Brown CT, Hug LA, Sharon I, Castelle CJ, Probst AJ, Thomas BC, Singh A, Wilkins MJ, Karaoz U, Brodie EL, Williams KH, Hubbard SS, Banfield JF. 2016. Thousands of microbial genomes shed light on interconnected biogeochemical processes in an aquifer system. Nat Commun 7:1–11. https://doi.org/10.1038/ncomms13219.
41. Rosewarne CP, Greenfield P., Li D, Tran-Dinh N, Midgley DJ, Hendry P. 2013. Draft genome sequence of *Methanobacterium* sp. Maddingley, reconstructed from metagenomic sequencing of a methanogenic microbial consortium enriched from coal-seam gas formation water. Genome Announc 1:e00082-12. https://doi.org/10.1128/genomeA.00082-12.
42. Dalcin Martins P, Danczak RE, Roux S, Frank J, Borton MA, Wolfe RA, Burris MN, Wilkins MJ. 2018. Viral and metabolic controls on high rates of microbial sulfur and carbon cycling in wetland ecosystems. Microbiome 6:1–17. https://doi.org/10.1186/s40168-018-0522-4.
43. Probst AJ, Ladd B, Jarett JK, Geller-McGrath DE, Sieber CMK, Emerson JB, Anantharaman K, Thomas BC, Malmstrom RR, Stieglmeier M, Klingl A, Woyke T, Ryan MC, Banfield JF. 2018. Differential depth distribution of microbial function and putative symbionts through sediment-hosted aquifers in the deep terrestrial subsurface. Nat Microbiol 3:328–336. https://doi.org/10.1038/s41564-017-0098-y.
44. Wilkins LGE, Ettinger CL, Jospin G, Eisen JA. 2019. Metagenome-assembled genomes provide new insights into two thermal pools in Kamchatka, Russia. Sci Rep 9:3059. https://doi.org/10.1038/s41598-019-39576-6.
45. He Y, Li M, Perumal V, Feng X, Fang J, Xie J, Sievert SM, Wang F. 2016. Genomic and enzymatic evidence for acetogenesis among multiple lineages of the archaeal phylum *Bathyarchaeota* widespread in marine sediments. Nat Microbiol 1:1–9. https://doi.org/10.1038/nmicrobiol.2016.35.
46. Yu T, Wu W, Liang W, Lever MA, Hinrichs K-U, Wang F. 2018. Growth of sedimentary *Bathyarchaeota* on lignin as an energy source. Proc Natl Acad Sci U S A 115:6022–6027. https://doi.org/10.1073/pnas.1718854115.
47. Evans PN, Parks DH, Chadwick GL, Robbins SJ, Orphan VJ, Golding SD, Tyson GW. 2015. Methane metabolism in the archaeal phylum *Bathyarchaeota* revealed by genome-centric metagenomics. Science 350:434–438. https://doi.org/10.1126/science.aac7745.
48. Xiang X, Wang R, Wang H, Gong L, Man B, Xu Y. 2017. Distribution of *Bathyarchaeota* communities across different terrestrial settings and their potential ecological functions. Sci Rep 7:1–11. https://doi.org/10.1038/srep45028.
49. Narrowe AB, Angle JC, Daly RA, Stefanik KC, Wrighton KC, Miller CS. 2017. High-resolution sequencing reveals unexplored archaeal diversity in freshwater wetland soils. Environ Microbiol 19:2192–2209. https://doi.org/10.1111/1462-2920.13703.
50. Webster G, Yarram L, Freese E, Köster J, Sass H, Parkes RJ, Weightman AJ. 2007. Distribution of candidate division JS1 and other bacteria in tidal sediments of the German Wadden Sea using targeted 16S rRNA gene PCR-DGGE. FEMS Microbiol Ecol 62:78–89. https://doi.org/10.1111/j.1574-6941.2007.00372.x.
51. Rastogi G, Osman S, Kukkadapu R, Engelhard M, Vaishampayan PA, Andersen GL, Sani RK. 2010. Microbial and mineralogical characterizations of soils collected from the deep biosphere of the former Homestake Gold Mine, South Dakota. Microb Ecol 60:539–550. https://doi.org/10.1007/s00248-010-9657-y.
52. Nobu MK, Dodsworth JA, Murugapiran SK, Rinke C, Gies EA, Webster G, Schwientek P, Kille P, Parkes RJ, Sass H, Jørgensen BB, Weightman AJ, Liu W-T, Hallam SJ, Tsiamis G, Woyke T, Hedlund BP. 2016. Phylogeny and physiology of candidate phylum 'Atribacteria' (OP9/JS1) inferred from cultivation-independent genomics. ISME J 10:273–286. https://doi.org/10.1038/ismej.2015.97.
53. Glass JB, Ranjan P, Kretz CB, Nunn BL, Johnson AM, McManus J, Stewart FJ. 2019. Adaptations of *Atribacteria* to life in methane hydrates: hot traits for cold life. bioRxiv https://doi.org/10.1101/536078.
54. Gies EA, Konwar KM, Beatty JT, Hallam SJ. 2014. Illuminating microbial dark matter in meromictic Sakinaw Lake. Appl Environ Microbiol 80:6807–6818. https://doi.org/10.1128/AEM.01774-14.
55. Dignac M-F, Bahri H, Rumpel C, Rasse DP, Bardoux G, Balesdent J, Girardin C, Chenu C, Mariotti A. 2005. Carbon-13 natural abundance as a tool to study the dynamics of lignin monomers in soil: an appraisal at the Closeaux experimental field (France). Geoderma 128:3–17. https://doi.org/10.1016/j.geoderma.2004.12.022.
56. Jacquiod S, Demanèche S, Franqueville L, Ausec L, Xu Z, Delmont TO, Dunon V, Cagnon C, Mandic-Mulec I, Vogel TM, Simonet P. 2014. Characterization of new bacterial catabolic genes and mobile genetic elements by high throughput genetic screening of a soil metagenomic library. J Biotechnol 190:18–29. https://doi.org/10.1016/j.jbiotec.2014.03.036.
57. Gupta A, Dutta A, Sarkar J, Panigrahi MK, Sar P. 2018. Low-abundance members of the *Firmicutes* facilitate bioremediation of soil impacted by highly acidic mine drainage from the Malanjkhand copper project, India. Front Microbiol 9:2882. https://doi.org/10.3389/fmicb.2018.02882.
58. Zhang X, Zhang D, Huang Y, Zhang K, Lu P. 2018. Simultaneous removal of organic matter and iron from hydraulic fracturing flowback water through sulfur cycling in a microbial fuel cell. Water Res 147:461–471. https://doi.org/10.1016/j.watres.2018.10.020.
59. Clavel T, Lepage P, Charrier C. 2014. The family *Coriobacteriaceae*, p 201–238. *In* Rosenberg E, DeLong EF, Lory S, Stackebrandt E, Thompson F (ed), The prokaryotes. Springer, Berlin, Germany.
60. Fu Q, Kuramochi Y, Fukushima N, Maeda H, Sato K, Kobayashi H. 2015. Bioelectrochemical analyses of the development of a thermophilic biocathode catalyzing electromethanogenesis. Environ Sci Technol 49:1225–1232. https://doi.org/10.1021/es5052233.

61. Traore SI, Yasir M, Azhar EI, Bibi F, Bittar F, Jiman-Fatani AA, Fournier P-E, Edouard S. 2016. *Raoultibacter massiliensis*" gen. nov., sp. nov., a new bacterium isolated from the human gut of a Saudi Bedouin. New Microbes New Infect 14:1–3. https://doi.org/10.1016/j.nmni.2016.06.013.
62. Van Der Kolk DA, Flaig PP, Hasiotis ST. 2015. Paleoenvironmental reconstruction of a late Cretaceous, muddy, river-dominated Polar deltaic system: Schrader Bluff-Prince Creek formation transition, Shivugak Bluffs, North Slope of Alaska, U.S.A. J Sediment Res 85:903–936. https://doi.org/10.2110/jsr.2015.58.
63. Daquiado AR, Kuppusamy S, Kim SY, Kim JH, Yoon Y-E, Kim PJ, Oh S-H, Kwak Y-S, Lee YB. 2016. Pyrosequencing analysis of bacterial community diversity in long-term fertilized paddy field soil. Appl Soil Ecol 108:84–91. https://doi.org/10.1016/j.apsoil.2016.08.006.
64. Noguchi M, Kurisu F, Kasuga I, Furumai H. 2014. Time-resolved DNA stable isotope probing links *Desulfobacterales*- and *Coriobacteriaceae*-related bacteria to anaerobic degradation of benzene under methanogenic conditions. Microbes Environ 29:191–199. https://doi.org/10.1264/jsme2.me13104.
65. Jackson BE, Bhupathiraju VK, Tanner RS, Woese CR, McInerney MJ. 1999. *Syntrophus aciditrophicus* sp. nov., a new anaerobic bacterium that degrades fatty acids and benzoate in syntrophic association with hydrogen-using microorganisms. Arch Microbiol 171:107–114. https://doi.org/10.1007/s002030050685.
66. Cheng L, Ding C, Li Q, He Q, Dai L-R, Zhang H. 2013. DNA-SIP reveals that *Syntrophaceae* play an important role in methanogenic hexadecane degradation. PLoS One 8:e66784. https://doi.org/10.1371/journal.pone.0066784.
67. Plugge CM, Zhang W, Scholten JCM, Stams AJM. 2011. Metabolic flexibility of sulfate-reducing bacteria. Front Microbiol 2:81. https://doi.org/10.3389/fmicb.2011.00081.
68. Conrad R, Claus P, Chidthaisong A, Lu Y, Fernandez Scavino A, Liu Y, Angel R, Galand PE, Casper P, Guerin F, Enrich-Prast A. 2014. Stable carbon isotope biogeochemistry of propionate and acetate in methanogenic soils and lake sediments. Org Geochem 73:1–7. https://doi.org/10.1016/j.orggeochem.2014.03.010.
69. Chauhan A, Ogram A, Reddy KR. 2004. Syntrophic-methanogenic associations along a nutrient gradient in the Florida Everglades. Appl Environ Microbiol 70:3475–3484. https://doi.org/10.1128/AEM.70.6.3475-3484.2004.
70. Lueders T, Manefield M, Friedrich MW. 2004. Enhanced sensitivity of DNA- and rRNA-based stable isotope probing by fractionation and quantitative analysis of isopycnic centrifugation gradients. Environ Microbiol 6:73–78. https://doi.org/10.1046/j.1462-2920.2003.00536.x.
71. Robbins SJ, Evans PN, Parks DH, Golding SD, Tyson GW. 2016. Genome-centric analysis of microbial populations enriched by hydraulic fracture fluid additives in a coal bed methane production well. Front Microbiol 7:731. https://doi.org/10.3389/fmicb.2016.00731.
72. Kirk MF, Wilson BH, Marquart KA, Zeglin LH, Vinson DS, Flynn TM, Kirk MF. 2015. Solute concentrations influence microbial methanogenesis in coal-bearing strata of the Cherokee Basin, USA. Front Microbiol 6:1287. https://doi.org/10.3389/fmicb.2015.01287.
73. Jetten MSM, Stams AJM, Zehnder A. 1990. Acetate threshold values and acetate activating enzymes in methanogenic bacteria. FEMS Microbiol Lett 73:339–344. https://doi.org/10.1111/j.1574-6968.1990.tb03958.x.
74. Stantscheff R, Kuever J, Rabenstein A, Seyfarth K, Dröge S, König H. 2014. Isolation and differentiation of methanogenic archaea from mesophilic corn-fed on-farm biogas plants with special emphasis on the genus *Methanobacterium*. Appl Microbiol Biotechnol 98:5719–5735. https://doi.org/10.1007/s00253-014-5652-4.
75. Kitamura K, Fujita T, Akada S, Tonouchi A. 2011. *Methanobacterium kanagiense* sp. nov., a hydrogenotrophic methanogen, isolated from rice-field soil. Int J Syst Evol Biol 61:1246–1252. https://doi.org/10.1099/ijs.0.026013-0.
76. Denonfoux J, Parisot N, Dugat-Bony E, Biderre-Petit C, Boucher D, Morgavi DP, Le Paslier D, Peyretaillade E, Peyret P. 2013. Gene capture coupled to high-throughput sequencing as a strategy for targeted metagenome exploration. DNA Res 20:185–196. https://doi.org/10.1093/dnares/dst001.
77. Joulian C, Ollivier B, Patel BKC, Roger PA. 1998. Phenotypic and phylogenetic characterization of dominant culturable methanogens isolated from ricefield soils. FEMS Microbiol Ecol 25:135–145. https://doi.org/10.1111/j.1574-6941.1998.tb00467.x.
78. Joulian C, Patel B, Ollivier B, Garcia JL, Roger PA. 2000. *Methanobacterium oryzae* sp. nov., a novel methanogenic rod isolated from a Philippines ricefield. Int J Syst Evol Microbiol 50:525–528. https://doi.org/10.1099/00207713-50-2-525.
79. Zellner G, Bleicher K, Braun E, Kneifel H, Tindall BJ, de Macario EC, Winter J. 1988. Characterization of a new mesophilic, secondary alcohol-utilizing methanogen, *Methanobacterium palustre* spec. nov. from a peat bog. Arch Microbiol 151:1–9. https://doi.org/10.1007/BF00444660.
80. Sakai S, Imachi H, Sekiguchi Y, Tseng I-C, Ohashi A, Harada H, Kamagata Y. 2009. Cultivation of methanogens under low-hydrogen conditions by using the coculture method. Appl Environ Microbiol 75:4892–4896. https://doi.org/10.1128/AEM.02835-08.
81. Lupton FS, Zeikus J. 1984. Physiological basis for sulfate-dependent hydrogen competition between sulfidogens and methanogens. Curr Microbiol 11:7–11. https://doi.org/10.1007/BF01567568.
82. Rotaru A-E, Shrestha M, Liu F, Markovaite B, Chen S, Nevin KP, Lovley R. 2014. Direct interspecies electron transfer between *Geobacter metallireducens* and *Methanosarcina barkeri*. Appl Environ Microbiol 80:4599–4605. https://doi.org/10.1128/AEM.00895-14.
83. Yee MO, Snoeyenbos-West OL, Thamdrup B, Ottosen LDM, Rotaru A-E. 2019. Extracellular electron uptake by two *Methanosarcina* species. Front Energy Res 7:1–10.
84. Jaramillo PAP, Snoeyenbos-West O, Loescher C, Thamdrup B, Rotaru A-E. 2019. Baltic *Methanosarcina* and *Clostridium* compete for electrons from metallic iron. bioRxiv https://doi.org/10.1101/530386.
85. Kühn W, Fiebig K, Hippe H, Mah RA, Huser BA, Gottschalk G. 1983. Distribution of cytochromes in methanogenic bacteria. FEMS Microbiol Lett 20:407–410. https://doi.org/10.1016/0378-1097(83)90105-2.
86. Walker DJF, Martz E, Holmes DE, Zhou Z, Nonnenmann SS, Lovley DR. 2019. The archaellum of *Methanospirillum hungatei* is electrically conductive. mBio 10:e00579-19. https://doi.org/10.1128/mBio.00579-19.
87. Albers S-V, Jarrell KF. 2015. The archaellum: how archaea swim. Front Microbiol 6:23. https://doi.org/10.3389/fmicb.2015.00023.
88. Liu F, Rotaru A-E, Shrestha PM, Malvankar NS, Nevin KP, Lovley DR. 2015. Magnetite compensates for the lack of a pilin-associated *c*-type cytochrome in extracellular electron exchange. Environ Microbiol 17:648–655. https://doi.org/10.1111/1462-2920.12485.
89. Tang Y-Q, Ji P, Hayashi J, Koike Y, Wu X-L, Kida K. 2011. Characteristic microbial community of a dry thermophilic methanogenic digester: its long-term stability and change with feeding. Appl Microbiol Biotechnol 91:1447–1461. https://doi.org/10.1007/s00253-011-3479-9.
90. Kotsyurbenko OR. 2005. Trophic interactions in the methanogenic microbial community of low-temperature terrestrial ecosystems. FEMS Microbiol Ecol 53:3–13. https://doi.org/10.1016/j.femsec.2004.12.009.
91. Sivan O, Shusta SS, Valentine DL. 2016. Methanogens rapidly transition from methane production to iron reduction. Geobiology 14:190–203. https://doi.org/10.1111/gbi.12172.
92. Kunapuli U, Lueders T, Meckenstock RU. 2007. The use of stable isotope probing to identify key iron-reducing microorganisms involved in anaerobic benzene degradation. ISME J 1:643–653. https://doi.org/10.1038/ismej.2007.73.
93. Reiche M, Torburg G, Küsel K. 2008. Competition of Fe(III) reduction and methanogenesis in an acidic fen. FEMS Microbiol Ecol 65:88–101. https://doi.org/10.1111/j.1574-6941.2008.00523.x.
94. Rissanen AJ, Karvinen A, Nykänen H, Peura S, Tiirola M, Mäki A, Kankaala P. 2017. Effects of alternative electron acceptors on the activity and community structure of methane-producing and consuming microbes in the sediments of two shallow boreal lakes. FEMS Microbiol Ecol 93:fix078. https://doi.org/10.1093/femsec/fix078.
95. Marquart KA, Haller BR, Paper JM, Flynn TM, Boyanov MI, Shodunke G, Gura C, Jin Q, Kirk MF. 2019. Influence of pH on the balance between methanogenesis and iron reduction. Geobiology 17:185–198. https://doi.org/10.1111/gbi.12320.
96. McCauley A, Jones C, Jacobsen J. 2017. Soil pH and organic matter. Montana State University Extension Service, Bozeman, MT. http://landresources.montana.edu/nm/documents/NM8.pdf.
97. Bushnell B. 2014. BBMap: a fast, accurate, splice-aware aligner. https://www.osti.gov/biblio/1241166.
98. Nurk S, Meleshko D, Korobeynikov A, Pevzner PA. 2017. metaSPAdes: a new versatile metagenomic assembler. Genome Res 27:824–834. https://doi.org/10.1101/gr.213959.116.
99. Li H, Durbin R. 2010. Fast and accurate long-read alignment with Burrows-Wheeler transform. Bioinformatics 26:589–595. https://doi.org/10.1093/bioinformatics/btp698.
100. Li H, Handsaker B, Wysoker A, Fennell T, Ruan J, Homer N, Marth G,

Abecasis G, Durbin R. 2009. The sequence alignment/map format and SAMtools. Bioinformatics 25:2078–2079. https://doi.org/10.1093/bioinformatics/btp352.
101. Graham ED, Heidelberg JF, Tully BJ. 2017. BinSanity: unsupervised clustering of environmental microbial assemblies using coverage and affinity propagation. PeerJ 5:e3035. https://doi.org/10.7717/peerj.3035.
102. Lu YY, Chen T, Fuhrman JA, Sun F. 2018. COCACOLA: binning metagenomic contigs using sequence COmposition, read CoverAge, CO-alignment and paired-end read LinkAge. Bioinformatics 33:791–798.
103. Alneberg J, Bjarnason BS, De Bruijn I, Schirmer M, Quick J, Ijaz UZ, Lahti L, Loman NJ, Andersson AF, Quince C. 2014. Binning metagenomic contigs by coverage and composition. Nat Methods 11:1144–1146. https://doi.org/10.1038/nmeth.3103.
104. Wu Y-W, Simmons BA, Singer SW. 2016. MaxBin 2.0: an automated binning algorithm to recover genomes from multiple metagenomic datasets. Bioinformatics 32:605–607. https://doi.org/10.1093/bioinformatics/btv638.
105. Kang DD, Froula J, Egan R, Wang Z. 2015. MetaBAT, an efficient tool for accurately reconstructing single genomes from complex microbial communities. PeerJ 3:e1165. https://doi.org/10.7717/peerj.1165.
106. Sieber CMK, Probst AJ, Sharrar A, Thomas BC, Hess M, Tringe SG, Banfield JF. 2018. Recovery of genomes from metagenomes via a dereplication, aggregation, and scoring strategy. Nat Microbiol 3:836–843. https://doi.org/10.1038/s41564-018-0171-1.
107. Parks DH, Imelfort M, Skennerton CT, Hugenholtz P, Tyson GW. 2015. CheckM: assessing the quality of microbial genomes recovered from isolates, single cells, and metagenomes. Genome Res 25:1043–1055. https://doi.org/10.1101/gr.186072.114.
108. Seemann T. 2014. Prokka: rapid prokaryotic genome annotation. Bioinformatics 30:2068–2069. https://doi.org/10.1093/bioinformatics/btu153.
109. Pruitt KD, Tatusova T, Maglott DR. 2018. NCBI Reference Sequence (RefSeq): a curated nonredundant sequence database of genomes, transcripts and proteins. Nucleic Acids Res 33:501–504.
110. Moriya Y, Itoh M, Okuda S, Yoshizawa AC, Kanehisa M. 2007. KAAS: an automatic genome annotation and pathway reconstruction server. Nucleic Acids Res 35:182–185.
111. Rutherford K, Parkhill J, Crook J, Horsnell T, Rice P, Rajandream M-A, Barrell B. 2000. Artemis: sequence visualization and annotation. Bioinformatics 16:944–945. https://doi.org/10.1093/bioinformatics/16.10.944.
112. In 't Zandt MH, Beckmann S, Rijkers R, Jetten MSM, Manefield M, Welte CU. 2018. Nutrient and acetate amendment leads to acetoclastic methane production and microbial community change in a non-producing Australian coal well. Microb Biotechnol 11:626–638. https://doi.org/10.1111/1751-7915.12853.
113. Palacios PA, Snoeyenbos-West O, Löscher CR, Thamdrup B, Rotaru A-E. 23 August 2019. Baltic Sea methanogens compete with acetogens for electrons from metallic iron. ISME J https://doi.org/10.1038/s41396-019-0490-0.
114. Prakash D, Chauhan SS, Ferry JG. 2019. Ferry JG. 2019. Life on the thermodynamic edge: respiratory growth of an acetotrophic methanogen. Sci Adv 5:eaaw9059. https://doi.org/10.1126/sciadv.aaw9059.
115. Tang H-Y, Holmes DE, Ueki T, Palacios PA, Lovely DR. 2019. Iron corrosion via direct metal-microbe electron transfer. mBio 10: e00303-19. https://doi.org/10.1128/mBio.00303-19.